Proc. Natl. Acad. Sci. USA
Vol. 96, pp. 1094–1099, February 1999
Neurobiology

A presynaptic role for the ADP ribosylation factor (ARF)-specific GDP/GTP exchange factor msec7-1

URI ASHERY*†, HENRIETTE KOCH†‡, VOLKER SCHEUSS*, NILS BROSE‡, AND JENS RETTIG*§

*Department of Membrane Biophysics, Max Planck Institute for Biophysical Chemistry, Am Fassberg 11, D-37077 Goettingen, Germany; and ‡Department of Neurobiology, Max Planck Institute for Experimental Medicine, Hermann-Rein-Strasse 3, D-37075 Goettingen, Germany

Communicated by Erwin Neher, Max Planck Institute for Biophysical Chemistry, Goettingen, Germany, November 30, 1998 (received for review September 15, 1998)

ABSTRACT **ADP ribosylation factors (ARFs) represent a family of small monomeric G proteins that switch from an inactive, GDP-bound state to an active, GTP-bound state. One member of this family, ARF6, translocates on activation from intracellular compartments to the plasma membrane and has been implicated in regulated exocytosis in neuroendocrine cells. Because GDP release *in vivo* is rather slow, ARF activation is facilitated by specific guanine nucleotide exchange factors like cytohesin-1 or ARNO. Here we show that msec7-1, a rat homologue of cytohesin-1, translocates ARF6 to the plasma membrane in living cells. Overexpression of msec7-1 leads to an increase in basal synaptic transmission at the *Xenopus* neuromuscular junction. msec7-1-containing synapses have a 5-fold higher frequency of spontaneous synaptic currents than control synapses. On stimulation, the amplitudes of the resulting evoked postsynaptic currents of msec7-1-overexpressing neurons are increased as well. However, further stimulation leads to a decline in amplitudes approaching the values of control synapses. This transient effect on amplitude is strongly reduced on overexpression of msec7-1E157K, a mutant incapable of translocating ARFs. Our results provide evidence that small G proteins of the ARF family and activating factors like msec7-1 play an important role in synaptic transmission, most likely by making more vesicles available for fusion at the plasma membrane.**

Monomeric G proteins of the ADP ribosylation factor (ARF) family regulate membrane traffic in various subcellular compartments of the cell (1). Activation of ARF proteins occurs by a switch from an inactive, GDP-bound to an active, GTP-bound state and is strongly facilitated by guanine nucleotide exchange factors (GEFs). Various ARF-specific GEFs like cytohesin-1, ARNO, and Gea1 have been cloned (2–4). Their central domain (sec7 domain) is responsible for their exchange activity and has a high homology to the yeast sec7p, a molecule that regulates vesicle budding from the Golgi apparatus (5, 6). They also possess an amino-terminal coiled-coil domain and a carboxyl-terminal pleckstrin-homology domain. The pleckstrin-homology domain mediates an enhancement of the GEF activity by its binding to phosphatidylinositol 4,5-bisphosphate (PIP2) (2, 7). Most members of the ARF family are localized to the Golgi apparatus, where their activation leads to the recruitment of coat proteins to the membrane (1). In contrast, the least conserved member of this family, ARF6, is localized to the cell periphery and translocates from endosomal compartments to the plasma membrane when activated (8–10). Therefore, it is likely that certain ARFs function in subcellular compartments other than the Golgi apparatus.

The exocytotic membrane traffic in axon terminals represents a specialized form of an endosome/plasma membrane cycle. In the axon terminal, transmitter is released by fusion of synaptic vesicles with the plasma membrane. Synaptic vesicles are formed by budding from early endosomal compartments. They then are filled with neurotransmitter and translocate to a specialized region of the plasma membrane, the active zone, where they dock and mature to a fusion competent state. Vesicles then fuse with the plasma membrane in response to an elevated intracellular calcium concentration (e.g., after an action potential). Vesicular protein and lipid components are retrieved by clathrin-mediated endocytosis and are recycled directly or via early endosomes (11, 12). Indeed, ARF6 recently has been implicated in regulated exocytosis in neuroendocrine cells (13).

We investigated a potential role for ARFs in synaptic transmission by microinjecting mRNA of msec7-1 (14), a rat homologue of the human cytohesin-1 (4), into the developing neuromuscular junction of *Xenopus*. Overexpression of this GEF should lead to a permanent activation of endogenous ARFs by shifting the equilibrium to its GTP-bound state. The observed increase in minifrequency and initial evoked postsynaptic current (EPSC) amplitude provide evidence that monomeric G proteins of the ARF family might indeed play a role in the presynaptic cycle of synaptic vesicles.

MATERIALS AND METHODS

Expression Vectors. Expression vectors for full length rat msec7-1 were generated by cloning previously published cDNA fragments (GenBank accession no. U83895) into pcDNA3 (Invitrogen). Rat ARF6 (GenBank accession no. L12385) was amplified from rat brain total cDNA by PCR and was cloned into pcDNA3 (Invitrogen). Mammalian expression vectors encoding full length msec7-1 and ARF6 in frame with GFP were constructed in pEGFP-N1 (CLONTECH) by using engineered PCR fragments that ensured reading frame conservation. The Glu 157 → Lys mutation in msec7-1 was generated by PCR using primers that carried the appropriate coding sequence substitution (GAG to AAG at position 544–546 of the msec7-1 cDNA). Expression vectors for *Xenopus* microinjection experiments were generated in pCS2+ (15) by shuttling the appropriate inserts from previously cloned pcDNA3 and pEGFP-N1 constructs.

Translocation Assays and Confocal Microscopy. Human embryonic kidney cells (HEK 293, a human fibroblast cell line) were grown on glass coverslips coated with 0.5% gelatine (16) and were transfected with either ARF6-GFP or msec7-1-GFP expression vectors. Alternatively, cells were cotransfected with a combination of either ARF6-GFP/msec7-1 or ARF6/msec7-1-GFP. Cells were incubated for 2 days at 37°C, were

The publication costs of this article were defrayed in part by page charge payment. This article must therefore be hereby marked "*advertisement*" in accordance with 18 U.S.C. §1734 solely to indicate this fact.

PNAS is available online at www.pnas.org.

Abbreviations: ARF, ADP ribosylation factor; GEF, GDP/GTP exchange factor; EPSC, evoked postsynaptic current; SSC, spontaneous synaptic current.

†U.A. and H.K. contributed equally to this work.
§To whom reprint requests should be addressed. e-mail: jrettig@gwdg.de.

washed twice with PBS, and were fixed with 3% paraformaldehyde in PBS. Coverslips were mounted onto slides with Fluoromount-G (Southern Biotechnology Associates). Fluorescent and transmitted light images were taken with a confocal laser-scanning system consisting of an SLM 410 Zeiss confocal microscope with a 40×-oil objective. The 488-nm line was used for excitation, and the emitted light was filtered through a 515-nm long-pass filter and was detected by a photomultiplier. Images of the HEK cells represent a single cross section of the middle of each cell. Images of *Xenopus* nerve cells were created by projection of 10 successive scans taken at 1-μm distances in the *z* axis. Fluorescence intensity at the cell body and varicosities was measured off line with locally written software in IGOR (WaveMetrix, Lake Oswego, OR). Regions of interest were defined as the shape of the cell body and varicosity, respectively. We considered a varicosity as a swelling along the axon usually in contact with a muscle cell. No significant differences were detected between neurons injected with msec7-1-GFP or msec7-1/GFP with respect to their varicosity size (1.52 and 1.34 μm^2, respectively), cell body size (18.9 and 23.3 μm^2, respectively), and number of varicosities per neuron (4 and 5, respectively). Therefore, we measured fluorescence intensity as absolute pixel values per region of interest, assuming no differences in height (*z* axis). The ratio of varicosity to soma fluorescence (f_R) was calculated for each cell independently, eliminating differences arising from different GFP expression levels in each cell. Values for f_R obtained for each cell were pooled, and the averaged f_R values for msec7-1-GFP or msec7-1/GFP containing neurons are displayed in Fig. 2*C*.

mRNA Injection. cDNAs of full length msec7-1, msec7-1-GFP, msec7-1E157K, and GFP in pCS2+ were linearized with *Not*I and were transcribed *in vitro* by using SP6 RNA Polymerase (Boehringer Mannheim). The resulting mRNAs were suspended in RNase-free H_2O to a final concentration of 2 $\mu g/\mu l$ each for msec7-1, msec7-1-GFP, and msec7-1E157K and 0.4 $\mu g/\mu l$ for GFP. The mRNA for msec7-1 or for msec7-1E157K was mixed with GFP mRNA, and ≈10 nl of that mixture were pressure injected into one blastomere of embryos at the 8- to 16-cell stage (Microinjector 5242; Eppendorf). Ten nanoliters of msec7-1-GFP were injected without further processing.

To determine the expression level of msec7-1 and msec7-1E157K constructs, we performed immunoblot analyses on individual injected and noninjected embryos at different developmental stages after injection by using a polyclonal antibody to msec7 (not shown). Both msec7-1 and msec7-1E157K were readily detectable at similar levels in 2- and 3-day-old embryos, indicating the presence of the proteins at times when electrophysiological measurements were performed. Likewise, msec7-1-GFP fluorescence was detected for several days after injection. Noninjected embryos showed weak msec7-1 immunoreactivity (at least 10× lower than injected embryos), indicating the presence of an endogenous msec7 homologue.

Preparation of Nerve–Muscle Cocultures and Electrophysiological Recordings. *Xenopus* nerve–muscle cocultures were prepared from the neural tube and associated myotomal tissue of stage 20–22 embryos as described (17, 18). Before recording, spinal neurons were examined for GFP fluorescence. A monochromator-based illumination system (T.I.L.L. Photonics, Martinsried, Germany) was coupled into the epifluorescence port of an inverted IM 35 microscope (Zeiss) by using a Fluar objective (40×, 1.3 n.a., oil immersion; Zeiss). Excitation wavelength for GFP was 488 nm, and the filter set was DC495, LP505 (T.I.L.L. Photonics).

GFP-containing fluorescent nerve cells were assumed to coexpress msec7-1 or msec7-1E157K, respectively. Synaptic currents were recorded from innervated muscle cells in the whole-cell configuration by using a combination of EPC-9 and EPC-7 amplifiers driven by the PULSE 8.12 software package

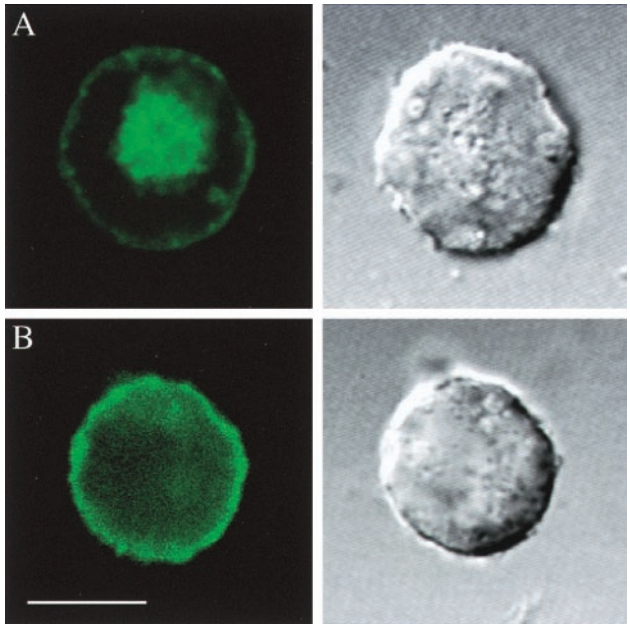

FIG. 1. Plasma membrane localization of ARF6/msec7-1 complex. HEK 293 cells were transfected with expression vectors of full length ARF6 with C-terminally attached GFP (ARF6-GFP) (*A*) or a combination of ARF6-GFP and msec7-1 (*B*). Confocal fluorescence images are displayed on the left; transmitted light images of the same cells are displayed on the right. While ARF6-GFP alone was associated mainly with endosomes and partially along the plasma membrane (*A*), the ARF6-GFP/msec7-1 complex was located almost exclusively to the plasma membrane (*B*). (Bar = 10 μm.)

(HEKA Electronics, Lambrecht/Pfalz, Germany). The pipette solution for the muscle cells contained 107 mM CsCl, 1 mM $MgCl_2$, 1 mM NaCl, 10 mM EGTA, and 10 mM Hepes (pH 7.3). The bath solution contained normal frog ringer (116 mM NaCl/2 mM KCl/1 mM $MgCl_2$/1.8 mM $CaCl_2$/5 mM Hepes, pH 7.3). The muscle cells routinely were clamped at −50 mV holding potential. A 10-ms test pulse to −60 mV was given before each sweep to estimate the series resistance for later offline series resistance compensation as described (18). The nerve cells were held at a potential between −50 and −70 mV in the current clamp mode. Trains of six action potentials with an interval of 25 ms were elicited every 4 s with 2-ms current injections of 900 pA. The pipette was filled with 114 mM K-gluconate, 10 mM KCl, 1 mM NaCl, 1 mM $MgCl_2$, 2 mM MgATP, 0.3 mM GTP, 50 μM fura-2, and 10 mM Hepes (pH 7.3). Amplitudes of EPSCs were analyzed with locally written software in IGOR as described (18). Spontaneous synaptic currents (SSCs) were recorded for a duration of 1–3 min while the recording chamber was perfused with 1–2 μM tetrodotoxin to prevent the generation of action potentials. Alternatively, the nerve cell was held in the current clamp mode, and possible action potential-evoked SSCs were eliminated from analysis. SSC amplitudes and frequencies were analyzed with locally written software in IGOR. Because we found no apparent differences in either SSC frequencies or EPSC amplitudes from msec7-1 and msec7-1-GFP-positive nerve cells, these data were pooled for analysis.

RESULTS AND DISCUSSION

To demonstrate that msec7-1 acts as a GEF on ARF6, we performed cotransfection experiments in HEK 293 cells. In agreement with previous reports (9–11, 19), transfection of a GFP-tagged ARF6 construct (ARF6-GFP) led to a broad fluorescence signal in endosomal compartments and at the plasma membrane (Fig. 1*A*). When cotransfected with

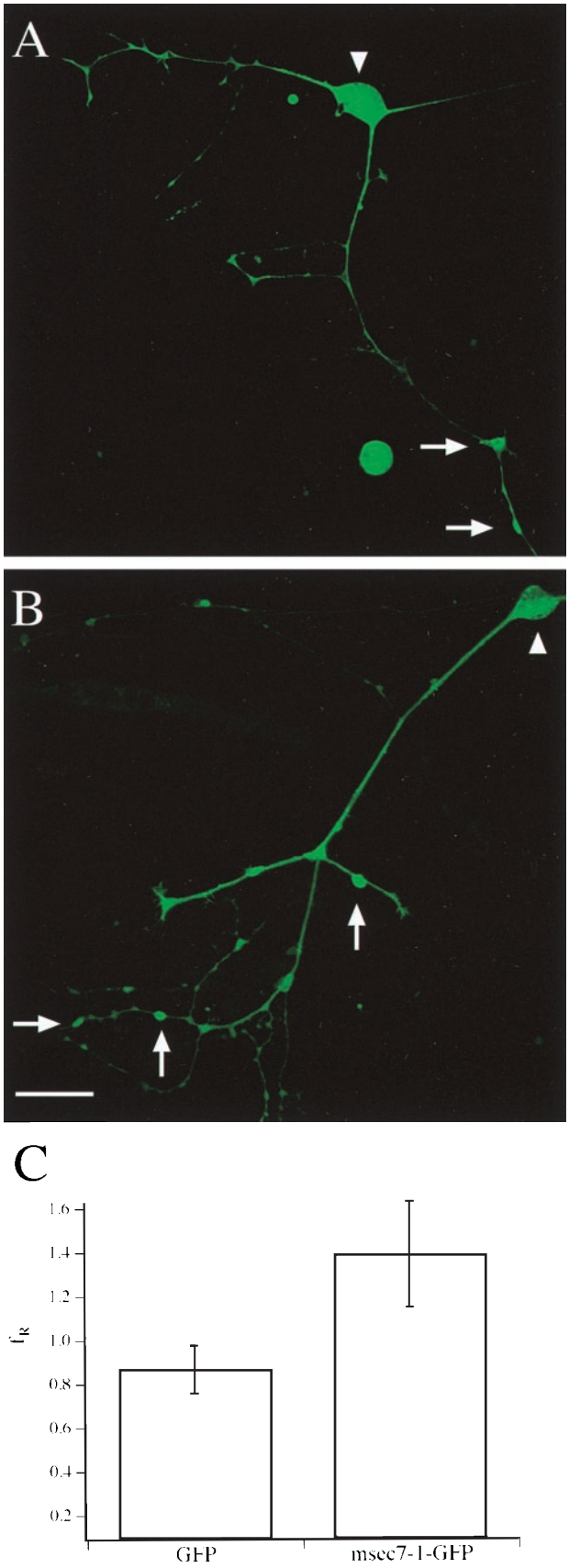

FIG. 2. msec7-1 is located predominantly to presynaptic regions of *Xenopus* nerve cells. Shown is the fluorescence pattern of spinal cord neurons injected with a mixture of msec7-1 and GFP mRNA (*A*) or with msec7-1-GFP mRNA (*B*). Note that the postsynaptic muscle cells in these examples are not visible because of their lack of GFP fluorescence. Arrows, varicosities; arrowheads, cell bodies. (Bar = 50 μm.) (*C*) Quantitative analysis of fluorescence intensities. The ratio of varicosity to soma fluorescence (f_R) in GFP and msec7-1-GFP containing neurons was 0.87 ± 0.11 (n = 8) and 1.39 ± 0.24 (n = 8), respectively. Error bars are given as SEM.

msec7-1, however, ARF6-GFP fluorescence was observed almost exclusively at the plasma membrane (Fig. 1*B*). In contrast, fluorescence images of cells cotransfected with ARF6-GFP and msec7-1E157K, the mutant used in overexpression experiments (see Fig. 4*D*), were indistinguishable from ARF6-GFP alone (not shown). Thus, msec7-1, but not its mutant msec7-1E157K, is capable of activating ARF6 by transferring it to its GTP-bound, plasma membrane-associated form. Identical results were obtained on cotransfection of GFP-tagged msec7-1 and ARF6 (not shown), confirming that the GFP at the C terminus does not interfere with the GEF function of msec7-1. Therefore, we investigated a potential role for msec7-1 in synaptic transmission by microinjecting either msec7-1-GFP mRNA or a mixture of msec7-1 and GFP mRNA into the developing neuromuscular junction of *Xenopus* (17, 18). In culture, msec7-1-expressing nerve cells were identified by GFP fluorescence (Fig. 2). We further tested whether msec7-1-GFP was preferentially localized to presynaptic areas of the nerve cells. Quantitative comparison of the fluorescence intensities of msec7-1-GFP and GFP alone revealed that msec7-1-GFP was ≈60% more enriched in varicosities and presynaptic regions of neurons compared with the soma (Fig. 2 *B* and *C*; n = 8). In contrast, neurons expressing GFP (and the untagged msec7-1) displayed a more uniform fluorescence distribution with higher intensities in the cell bodies (Fig. 2 *A* and *C*; n = 8). This subcellular localization pattern suggests a presynaptic function for msec7-1 in addition to the established role in activation of ARF proteins in the Golgi (1).

To address a potential role for msec7-1 in synaptic transmission, we first compared the basal release properties of msec7-1-containing synapses to that of control synapses. For this purpose, we measured SSCs from muscle cells innervated either by control or by msec7-1-containing neurons. (Fig. 3*A*). As summarized in Fig. 3*B*, the frequency of SSCs in msec7-1-containing synapses was ≈5-fold higher than that of control synapses. In contrast, the mean SSC amplitude was comparable to that of controls (Fig. 3*C*), suggesting that overexpression of msec7-1 leads to an increase in number, not in size, of releasable synaptic vesicles at the active zone. On the light microscopy level, the number and size of synaptic terminals was unaltered between injected and noninjected neurons (not shown), arguing against a possible role of msec7-1 in synapse development.

If the number of releasable vesicles is increased in msec7-1-overexpressing synapses, the postsynaptic responses after action potential-evoked release should be enlarged as well. We tested this assumption by inducing action potentials on the nerve cell soma and simultaneously measuring the EPSCs on the connected muscle cell (see *Materials and Methods* for details). As exemplified in Fig. 4*A*, we observed a fast rundown in EPSC amplitude on repetitive stimulation (six stimuli at 40 Hz every 4 s). The rundown occurred in two steps, an initial fast rundown with a time constant τ of 14.2 s and a slower phase with a time constant τ of 111 s. The latter time constant was comparable to that of the basal rundown observed in control cells (Fig. 4 *B* and *C*). Furthermore, a comparison of averaged EPSC amplitudes from msec7-1-containing (8.6 nA; n = 26) and control (6.0 nA; n = 27) synapses revealed that the initial amplitudes at the beginning of the experiments were significantly higher for injected cells (Fig. 4*B*). On prolonged stimulation, however, these amplitudes declined and became indistinguishable from those of control cells (Fig. 4*B*). This phenomenon suggests that the rundown effect is of presynaptic

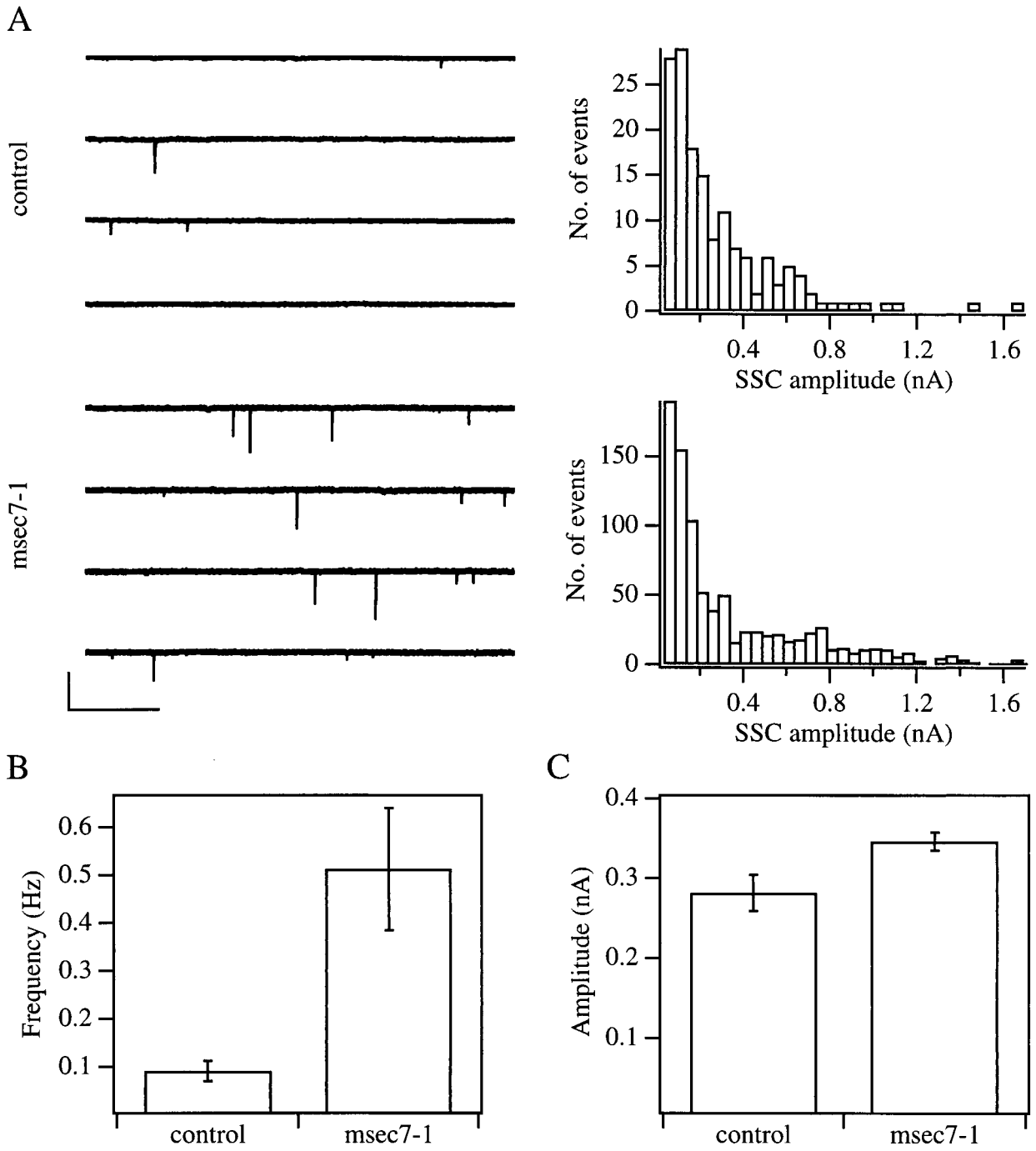

FIG. 3. msec7-1 expressing synapses have a higher frequency of spontaneous synaptic currents. (*A*) Representative traces of SSCs recorded from muscle cells that were innervated either by a control neuron (upper left) or by an msec7-1-containing neuron (lower left). The currents on the muscle cells are shown as downward deflections and represent single SSCs. (Bars = 0.5 s and 0.5 nA.) The corresponding amplitude distributions of the SSCs are shown on the right. (*B* and *C*) Summary of SSC frequency (*B*) and amplitude (*C*) of control and msec7-1-containing synapses. The average SSC frequency was 0.1 ± 0.02 Hz in control neurons (mean ± SEM; 153 SSCs, 13 cells) and 0.5 ± 0.12 Hz in msec7-1 neurons (mean ± SEM; 892 SSCs, 17 cells). The average SSC amplitude was 281 ± 22.7 pA and 345 ± 11.5 pA (mean ± SEM) for control and msec7-1 neurons, respectively. Error bars are given as SEM.

origin representing an initially larger vesicle pool that approaches the control pool size on repetitive stimulation. In Fig. 4*C*, the averaged EPSC amplitudes are normalized to the respective first amplitude in each experiment to demonstrate the fast rundown of the EPSC amplitude in msec7-1 synapses.

We next investigated whether the observed effect of msec7-1 overexpression was attributable to the GEF activity on ARFs. We took advantage of the recent crystallization data of the sec7 domain of ARNO (20, 21). A point mutation in this ARF binding domain (E156K) virtually abolishes activation of ARF by ARNO. We generated a construct bearing this point mutation (msec7-1-mut) and performed the identical stimulation protocol on msec7-1-mut-containing synapses. As summarized in Fig. 4*D*, the averaged, normalized amplitudes of msec7-1-mut-containing cells declined significantly slower than msec7-1 neurons (compare Fig. 4*D*, filled squares to Fig. 4*C*, filled circles). We, therefore, conclude that the stimulatory effect of msec7-1 on synaptic transmission is mainly attributable to its GEF activity on presynaptic ARFs. However, there was still some, although not statistically significant, degree of

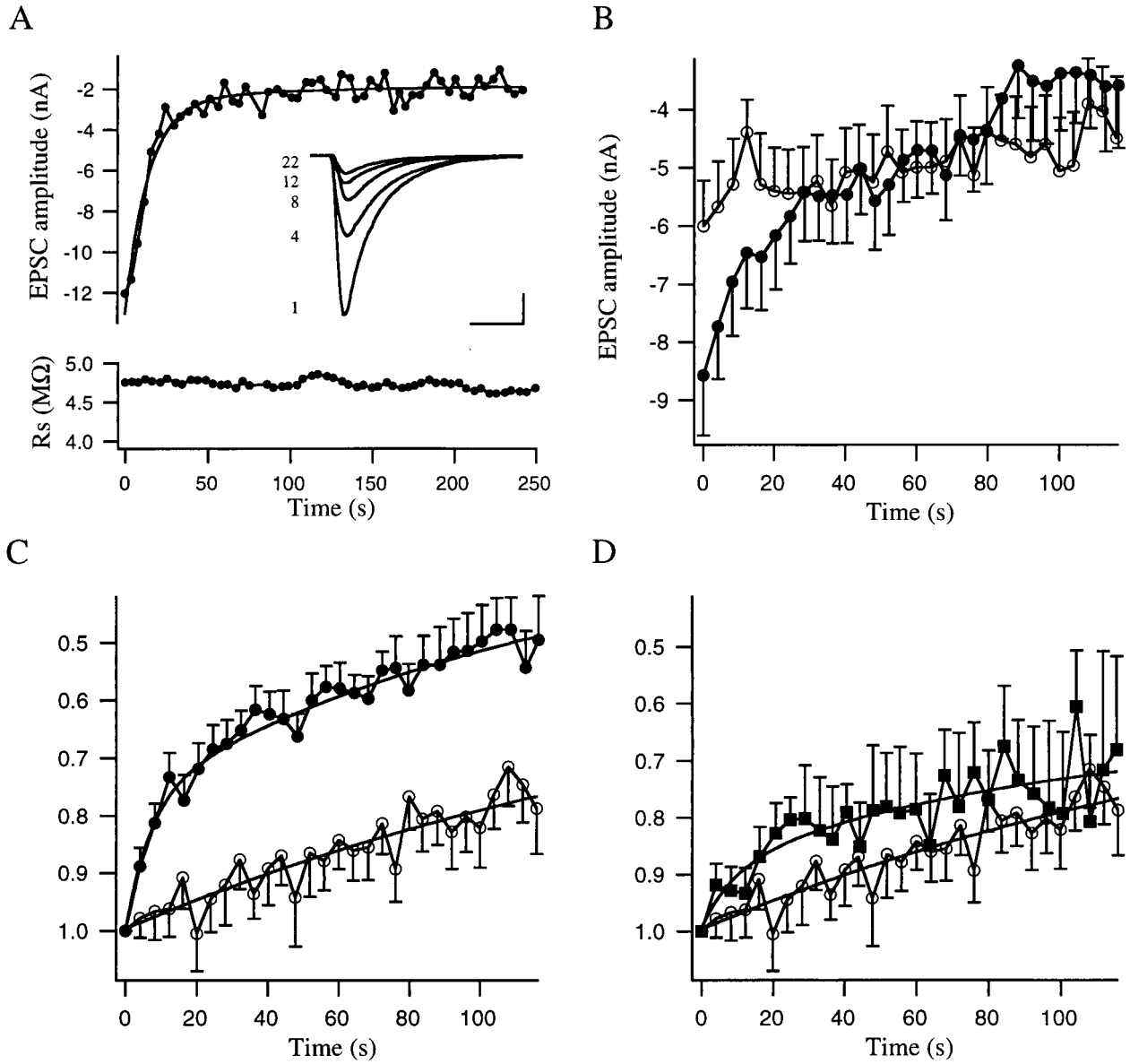

FIG. 4. Initial EPSC amplitudes are increased in msec7-1-containing synapses. (*A*) Representative experiment of an msec7-1-containing synapse. Trains of six action potentials were elicited on the nerve cell soma, and the resulting EPSCs were recorded from the innervated muscle cell. Data points represent the average amplitude of the EPSCs obtained during each train. The apparent fast rundown in amplitude is also evident from raw traces of first EPSCs in the indicated trains (*Inset*). (Bars = 5 ms and 5 nA.) The lower panel illustrates the series resistance values recorded from the muscle cell during the experiment. (*B*) Averaged, absolute EPSC amplitudes of control (open circles; $n = 27$) and msec7-1-containing synapses (filled circles; $n = 26$). Each data point represents the mean value of six EPSC amplitudes obtained during each train averaged for all experiments. (*C*) Same data as in *B* normalized to the first amplitude. The rundown in msec7-1 neurons has time constants of 15.7 and 125 s whereas in control cells the rundown is much slower and could be fitted with one exponential with a time constant of 180 s. (*D*) Comparison of averaged EPSC amplitudes, normalized to the first amplitude, of control (open circles; $n = 27$) and msec7-1-mut-containing synapses (filled squares; $n = 13$). Notably, no statistically significant difference in rundown of EPSC amplitudes could be observed between control and msec7-1-mut cells. Error bars are given as SEM.

rundown in these cells compared with control cells (Fig. 4*D*), indicating that msec7-1 without its GDP/GTP exchange activity might still have an influence on release. Potential mediators of this residual effect might be the N-terminal coiled-coil domain, which interacts with other synaptic proteins (N.B., unpublished work), or the C-terminal pleckstrin homology domain, which regulates GEF activity by interaction with phospholipids (2, 7).

Taken together, our data imply that another class of monomeric G proteins besides the Rab family (22) plays an important role in the presynaptic cycle of synaptic vesicles. Based on its subcellular localization, we consider ARF6 as the most likely candidate. Further work will have to clarify which member of the ARF family is located in the presynapse and whether the stimulatory effect of ARF-specific GDP/GTP exchange factors like msec7-1 is exclusively attributable to its action on ARF6 or whether other members of this growing family of G proteins are involved.

We thank Anke Bührmann and Sally Wenger for expert technical assistance, Dr. Christian Heinemann for initial contributions, and Dr. Erwin Neher for generous support. This investigation was supported by the Deutsche Forschungsgemeinschaft (N.B. and J.R.) and the Human Frontiers Science Program (U.A.).

1. Rothman, J. E. & Wieland, F. T. (1996) *Science* **272,** 227–234.
2. Chardin, P., Paris, S., Antonny, B., Robineau, S., Béraud-Dufour, S., Jackson, C. L. & Chabre, M. (1996) *Nature (London)* **384,** 481–484.

3. Peyroche, A., Paris, S. & Jackson, C. L. (1996) *Nature (London)* **384,** 479–481.
4. Meacci, E., Tsai, S.-C., Adamik, R., Moss, J. & Vaughan, M. (1997) *Proc. Natl. Acad. Sci. USA* **94,** 1745–1748.
5. Achstetter, T. A., Franzusoff, A., Field, C. & Schekman, R. (1988) *J. Biol. Chem.* **263,** 11711–11717.
6. Rambourg, A., Clermont, Y. & Kepes, F. (1993) *Anat. Rec.* **237,** 441–452.
7. Paris, S., Béraud-Dufour, S., Robineau, S., Bigay, J., Antonny, B., Chabre, M. & Chardin, P. (1997) *J. Biol. Chem.* **272,** 22221–22226.
8. D'Souza-Schorey, C., Li, G., Colombo, M. I. & Stahl, P. D. (1995) *Science* **267,** 1175–1178.
9. D'Souza-Schorey, C., van Donselaar, E., Hsu, V. W., Yang, C., Stahl, P. D. & Peters, P. J. (1998) *J. Cell Biol.* **140,** 603–616.
10. Peters, P. J., Hsu, V. W., Ooi, C. E., Finazzi, D., Teal, S. B., Oorschot, V., Donaldson, J. G. & Klausner, R. D. (1995) *J. Cell Biol.* **128,** 1003–1017.
11. Südhof, T. C. (1995) *Nature (London)* **375,** 645–653.
12. Murthy, V. N. & Stevens, C. F. (1998) *Nature (London)* **392,** 497–501.
13. Galas, M.-C., Helms, J. B., Vitale, N., Thiersé, D., Aunis, D. & Bader, M.-F. (1997) *J. Biol. Chem.* **272,** 2788–2793.
14. Telemenakis, I., Benseler, F., Stenius, K., Südhof, T. C. & Brose, N. (1997) *Eur. J. Cell Biol.* **74,** 143–149.
15. Rupp, R. A., Snider, L. & Weintraub, H. (1994) *Genes Dev.* **8,** 1311–1323.
16. Schnittler, H.-J., Franke, R. P., Akbay, U., Mrowietz, C. & Drenkhahn, D. (1993) *J. Physiol.* **265,** C289–C298.
17. Tabti, N. & Poo, M.-m. (1991) in *Culturing Nerve Cells*, eds. Banker, G. & Goslin, K. (MIT Press, Cambridge, MA), pp. 137–154.
18. Rettig, J., Heinemann, C., Ashery, U., Sheng, Z.-H., Yokoyama, C. T., Catterall, W. A. & Neher, E. (1997) *J. Neurosci.* **17,** 6647–6656.
19. Frank, S., Upender, S., Hansen, S. H. & Casanova, J. E. (1998) *J. Biol. Chem.* **273,** 23–27.
20. Cherfils, J., Ménétry, J., Mathieu, M., LeBras, G., Robineau, S., Béraud-Dufour, S., Antonny, B. & Chardin, P. (1998) *Nature (London)* **392,** 101–105.
21. Mossessova, E., Gulbis, J. M. & Goldberg, J. (1998) *Cell* **92,** 415–423.
22. Südhof, T. C. (1997) *Neuron* **18,** 519–522.